



Missouri University of Science and Technology
Scholars' Mine

International Conferences on Recent Advances
in Geotechnical Earthquake Engineering and
Soil Dynamics

1991 - Second International Conference on
Recent Advances in Geotechnical Earthquake
Engineering & Soil Dynamics

14 Mar 1991, 2:00 pm - 3:30 pm

Three Dimensional Wave Propagation due to Pile Driving

S. Savidis

Technical University, Berlin, Germany

A. Mitakidis

Consulting Engineer, Berlin, Germany

Follow this and additional works at: <https://scholarsmine.mst.edu/icrageesd>

 Part of the [Geotechnical Engineering Commons](#)

Recommended Citation

Savidis, S. and Mitakidis, A., "Three Dimensional Wave Propagation due to Pile Driving" (1991).
*International Conferences on Recent Advances in Geotechnical Earthquake Engineering and Soil
Dynamics*. 9.

<https://scholarsmine.mst.edu/icrageesd/02icrageesd/session10/9>

This Article - Conference proceedings is brought to you for free and open access by Scholars' Mine. It has been accepted for inclusion in International Conferences on Recent Advances in Geotechnical Earthquake Engineering and Soil Dynamics by an authorized administrator of Scholars' Mine. This work is protected by U. S. Copyright Law. Unauthorized use including reproduction for redistribution requires the permission of the copyright holder. For more information, please contact scholarsmine@mst.edu.



Three Dimensional Wave Propagation due to Pile Driving

S. Savidis

Professor of Soil Mechanics and Foundation Engineering, Technical University, Berlin, Germany

A. Mitakidis

Consulting Engineer, Berlin

SYNOPSIS: A very economical and efficient method to construct pile foundations or sheet walls is given by the driving of the pile itself in the case of prefabricated piles or of the steel-sheet pipe for concrete piles in situ and also by the driving of the sheet piles in the case of sheet walls. In spite of its efficiency this method underlies, because of environment protection reasons to certain restrictions, that concern the influence of the produced shock waves during the driving procedure to neighboring buildings and constructions. For the theoretical calculation of this influence at first the free-field response of the ground due to the propagated shock waves will be required. The source wave is generally of transient nature. The authors deal in this contribution with the theoretical calculation of free-field magnitudes for an elastic homogeneous half-space as an adequate model for an idealized ground.

INTRODUCTION

The problem of the three dimensional wave propagation in elastic media and particularly in those media restricted by a natural boundary, as the elastic half-space by its surface, has been intensively investigated in the last years by many authors. The most of the known solutions appears in the frequency domain. Johnson, 1974, yields the first analytical and complete solution of the problem in time domain. Although the solution is mathematically complex the expressions obtained there are very simple. Because of some slight but essential mistakes in the solution of Johnson, Mitakidis, 1989, resolved the three dimensional boundary value problem following the work and the solution technics of Johnson. The solution represents exact and in mathematically closed form evaluated Green's functions for the elastic half-space which are pointed out by an absolutely stable behavior in their numerical treatment.

SOLUTION OF THE PROBLEM IN TIME DOMAIN

The problem of the three dimensional wave propagation in the elastic homogeneous half-space consists in the solution of the Lamé-Navier equation of motion.

$$\rho \frac{\partial^2 \mathbf{u}(\mathbf{x}, t)}{\partial t^2} = \mathbf{f}(\mathbf{x}, t) + (\lambda + \mu) \nabla(\nabla \cdot \mathbf{u}(\mathbf{x}, t)) + \mu \Delta \mathbf{u}(\mathbf{x}, t) \quad (1)$$

In eq. (1) is \mathbf{u} the displacement vector, \mathbf{x} the location vector to the considered point A in the interior of the half-space, \mathbf{f} displays the force as source for the propagated elastic disturbance at the source point Q. The infinite elastic medium is given by its Lamé constants λ and μ , Fig. 1. In order to proceed in the solution of eq. (1), the source function \mathbf{f} , a single point load in the interior of the half-space will be localized in time and space with Dirac-delta functions:

$$\mathbf{f}(\mathbf{x}, t) = (F_1 \mathbf{e}_1 + F_2 \mathbf{e}_2 + F_3 \mathbf{e}_3) \delta(x_1 - X_1) \delta(x_2 - X_2) \delta(x_3 - X_3) \delta(t - T) \quad (2)$$

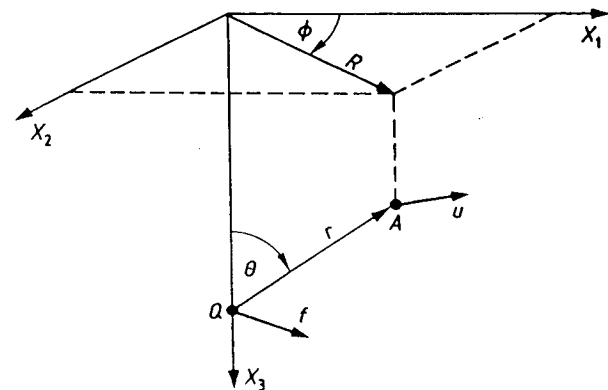


Fig. 1: Geometry of the problem: displacement \mathbf{u} at point A due to force \mathbf{f} at a point Q

In eq. (2) x_1, x_2, x_3 and t corresponds to the location and the arrival time of the disturbance at the controll point A, X_1, X_2, X_3 and T corresponds to the location and the moment of applying of the force \mathbf{f} at the source point Q. For a force vector, as given by eq. (2) the solution of eq. (1) corresponds to a Green's function so that we can write

$$\mathbf{u}(\mathbf{x}, t) = \mathbf{g}(\mathbf{x}, t; \mathbf{X}, T) \quad (3)$$

$$= g_1(\mathbf{x}, t; \mathbf{X}, T) \mathbf{e}_1 + g_2(\mathbf{x}, t; \mathbf{X}, T) \mathbf{e}_2 + g_3(\mathbf{x}, t; \mathbf{X}, T) \mathbf{e}_3$$

Physically $\mathbf{g}(\mathbf{x}, t; \mathbf{X}, T)$ means the displacement vector at moment t at the controll point A with location vector $\mathbf{x} = (x_1, x_2, x_3)$ due to an impulsive single point load \mathbf{F} applied at time T at the source point Q with location vector $\mathbf{X} = (X_1, X_2, X_3)$.

The eq. (1) is solved analytically by the aid of the Cagniard-De Hoop transform technic, Mitakidis 1989, accordingly to the work of

Johnson, 1974. The complete solution will be represented here for the case $X_3 = 0$, Point A at the surface, because the most interesting phenomena take place at the surface of the ground. For this case the solution has the form:

$$\mathbf{G} = \begin{bmatrix} G_{11} & G_{12} & G_{13} \\ G_{21} & G_{22} & G_{23} \\ G_{31} & G_{32} & G_{33} \end{bmatrix} \mathbf{F} \quad (4)$$

where

$$\mathbf{G} = \mathbf{G}^P + \mathbf{G}^S \quad (5)$$

The upper indices P and S in (5) characterize the P- and S-wave parts respectively of which consist the solution vector \mathbf{G} . For the problem considered here only the two components G_{13} and G_{33} will be used. After Mitakidis, 1989, they have the following form:

$$G_{13}^P = \frac{1}{n^2 \mu r} \frac{\partial}{\partial t} \int_0^{\rho} U(t - \frac{r}{v_p}) \operatorname{Re} \left\{ \frac{2q \eta_p \eta_s \cos \phi}{\sigma \left(\frac{t^2}{r^2} - \frac{1}{v_p^2} - \rho^2 \right)^{1/2}} \right\} dp \quad (6)$$

$$G_{33}^P = \frac{1}{n^2 \mu r} \frac{\partial}{\partial t} \int_0^{\rho} U(t - \frac{r}{v_p}) \operatorname{Re} \left\{ \frac{\eta_p \gamma}{\sigma \left(\frac{t^2}{r^2} - \frac{1}{v_p^2} - \rho^2 \right)^{1/2}} \right\} dp \quad (7)$$

In the case of steep radiation: $\sin \vartheta \ll v_s/v_p$

$$G_{13}^S = \frac{1}{n^2 \mu r} \frac{\partial}{\partial t} \int_0^{\rho} U(t - \frac{r}{v_s}) \operatorname{Re} \left\{ \frac{-\eta_s q \gamma \cos \phi}{\sigma \left(\frac{t^2}{r^2} - \frac{1}{v_s^2} - \rho^2 \right)^{1/2}} \right\} dp \quad (8)$$

$$G_{33}^S = \frac{1}{n^2 \mu r} \frac{\partial}{\partial t} \int_0^{\rho} U(t - \frac{r}{v_s}) \operatorname{Re} \left\{ \frac{2\eta_s \eta_p (q^2 - \rho^2)}{\sigma \left(\frac{t^2}{r^2} - \frac{1}{v_s^2} - \rho^2 \right)^{1/2}} \right\} dp \quad (9)$$

In the case of flat radiation $\sin \vartheta > v_s/v_p$

and $t > r \sqrt{\rho^2 + \frac{1}{v_s^2}}$ are

$$G_{13}^S = \frac{1}{n^2 \mu r} \frac{\partial}{\partial t} \int_0^{\rho} U(t - t_1) \operatorname{Re} \left\{ \frac{-\eta_s q \gamma \cos \phi}{\sigma \left(\frac{t^2}{r^2} - \frac{1}{v_s^2} - \rho^2 \right)^{1/2}} \right\} dp \quad (10)$$

$$G_{33}^S = \frac{1}{n^2 \mu r} \frac{\partial}{\partial t} \int_0^{\rho} U(t - t_1) \operatorname{Re} \left\{ \frac{2\eta_s \eta_p (q^2 - \rho^2)}{\sigma \left(\frac{t^2}{r^2} - \frac{1}{v_s^2} - \rho^2 \right)^{1/2}} \right\} dp \quad (11)$$

For $t < r \sqrt{\rho^2 + \frac{1}{v_s^2}}$ eqs. (11) and (12) become the form:

$$G_{13}^S = \frac{1}{n^2 \mu r} \frac{\partial}{\partial t} \int_0^{\rho} U(t - t_1) \operatorname{Im} \left\{ \frac{\eta_s q \gamma \cos \phi}{\sigma \left(\frac{1}{v_s^2} + \rho^2 - \frac{t^2}{r^2} \right)^{1/2}} \right\} dp \quad (12)$$

$$G_{33}^S = \frac{1}{n^2 \mu r} \frac{\partial}{\partial t} \int_0^{\rho} U(t - t_1) \operatorname{Im} \left\{ \frac{-2\eta_p \eta_s (q^2 - \rho^2)}{\sigma \left(\frac{1}{v_s^2} + \rho^2 - \frac{t^2}{r^2} \right)^{1/2}} \right\} dp \quad (13)$$

In the above eqs. (6) ./ (13) the following symbols have been used:

$U(t)$: is the Heaviside's unit step function

$$P_p = \left(\frac{t^2}{r^2} - \frac{1}{v_p^2} \right)^{1/2}$$

$$P_s = \left(\frac{t^2}{r^2} - \frac{1}{v_s^2} \right)^{1/2}$$

$$V_p = \left(\frac{2(1-\nu)\mu}{(1-2\nu)\rho} \right)^{1/2} \quad \text{Longitudinal wave velocity}$$

$$V_s = \left(\frac{\mu}{\rho} \right)^{1/2} \quad \text{shear wave velocity}$$

$$\eta_s = \left(\frac{1}{v_s^2} + \rho^2 - q^2 \right)^{1/2}; \quad \eta_p = \left(\frac{1}{v_p^2} + \rho^2 - q^2 \right)^{1/2}$$

$$\gamma = \eta_s^2 + \rho^2 - q^2; \quad \sigma = \gamma^2 + 4\eta_p \eta_s (q^2 - \rho^2)$$

$$\rho_1 = \left[\left(\frac{t}{r} - \left(\frac{1}{v_s^2} - \frac{1}{v_p^2} \right)^{1/2} \cos \vartheta \right) - \frac{1}{v_p^2} \right]^{1/2}$$

$$t_1 = \frac{r}{v_p} \sin \vartheta + r \left(\frac{1}{v_s^2} - \frac{1}{v_p^2} \right)^{1/2} \cos \vartheta$$

For the components with upper index p the separation variable q is given by

$$q = -\frac{t}{r} \sin \vartheta + i \left(\frac{t^2}{r^2} - \frac{1}{v_p^2} - \rho^2 \right)^{1/2} \cos \vartheta \quad (14)$$

In eqs. (8), (9), (12) and (13) q is given by

$$q = -\frac{t}{r} \sin \vartheta + i \left(\frac{t^2}{r^2} - \frac{1}{v_s^2} - \rho^2 \right)^{1/2} \cos \vartheta \quad (15)$$

Finally in eqs. (10) and (11) q has the form

$$q = -\frac{t}{r} \sin \vartheta + \left(\frac{1}{v_s^2} - \frac{t^2}{r^2} + \rho^2 \right)^{1/2} \cos \vartheta \quad (16)$$

By omitting the differentiation after the time the expression in eq. (6) till (13) yield the response of the half-space surface to a Heaviside unit-step function, Fig. 2 ./ 4.

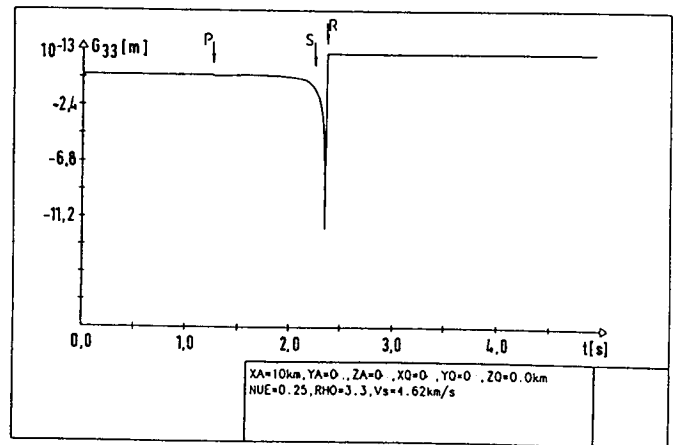


Fig.2a: Green's function G_{33}
Excitation of the half-space surface
Heaviside's unit step-function

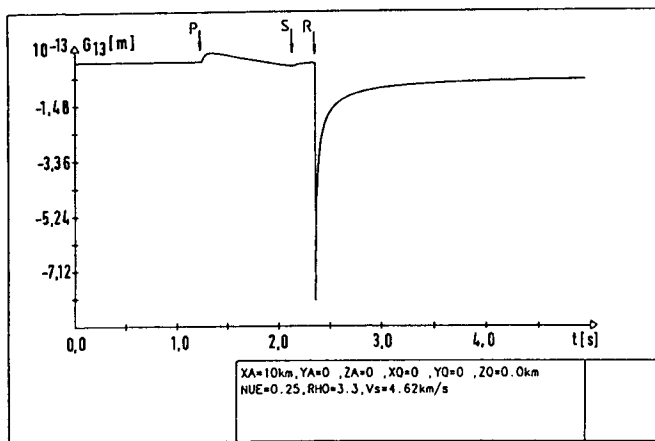


Fig. 2b: Greens's function G_{13}

Excitation of the half-space surface by Heavivide's unit step function

Figure 2 shows the surface behavior of the half space due to the Heavivide's unit step function acting at the half-space surface. The epicentral distance X_A of the controll point A has been chosen to be 10 km, the Poisson ratio ν of the medium amounts 0,25, the density $\rho = 3.3 \text{ t/m}^3$ (rock material) and the shear wave velocity is $v_s = 4.62 \text{ km/s}$.

All the three wave types of the half-space occur very clearly and they are pointed out by the symbols P for the Longitudinal wave, S for the shear wave and R for the well known Rayleigh-wave.

In Figure 3 the source of the elastic disturbance moves from the surface to a depth of $Z_Q = 2.0 \text{ km}$. All the other parameters remain the same. This is the case of flat-radiation.

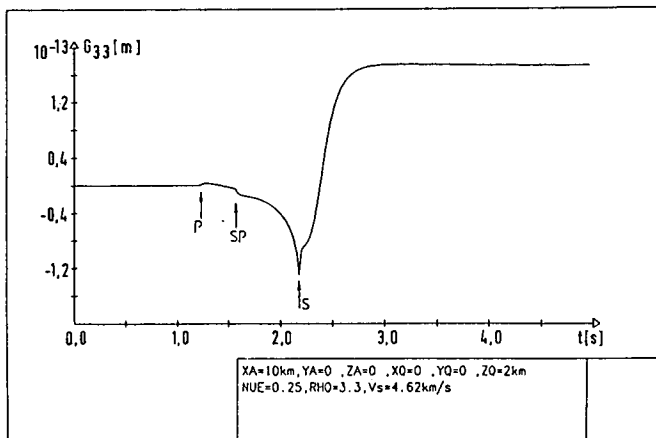


Fig. 3a: Green's function G_{33}

Hypocentral distance $Z_Q = 2.0 \text{ km}$

Epicentral distance $X_A = 10.0 \text{ km}$

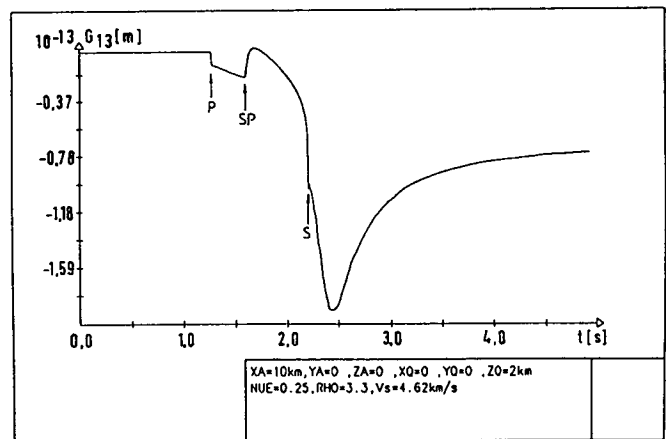


Fig. 3b: Green's function G_{13}

In Figure 3 we can see, that a very interesting phenomenon occurs as the wave source leaves the surface of the half-space: The main signal of the arriving R-wave disappears and another signal between the P- and S-Wave appears. This is the refracted at the surface of the half-space SP-Wave. The SP-Wave, or also known as head wave, occurs only in the case of flat radiation, it means in the case, that the radiation angle satisfy the condition: $\sin \theta > v_s/v_p$, Fig. 1. Finally in Fig. 4 the source lies in a depth of $Z_Q = 10 \text{ km}$ and the epicentral distance of the considered point A amounts 2 km. Here we have the case of steep radiation, $\sin \theta < v_s/v_p$, for which only the two main wave types P+S exist.

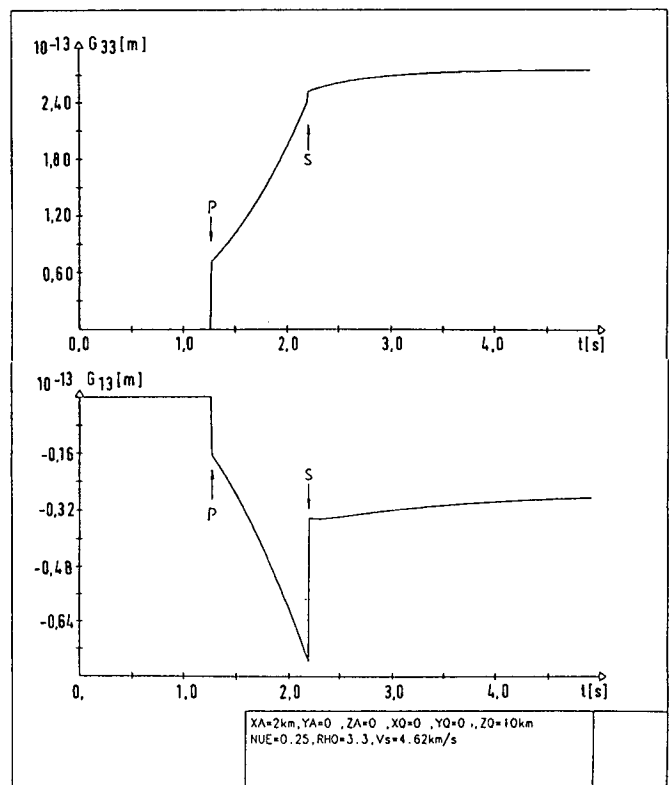


Fig. 4a: Green's function G_{33}

4b: Green's function G_{13}

SYSTEM RESPONSE TO ARBITRARY TRANSIENT LOADS

Because of the fact that the Green's function represents also the transfer function of the system half-space, they can be used to calculate by the aid of the Duhamel's convolution integral the system response to any arbitrary transient load, eq. (17).

$$\chi(t) = \int_0^t \frac{df(t-\tau)}{d\tau} g(\tau) d\tau \quad (17)$$

X(t): System response at time t

f(t): Load function

g(t): Transfer function of the considered system, must be known.

For the considered system of the elastic homogeneous half-space we obtain

$$W_{ij}(t) = \int_0^t \frac{df_i(t-\lambda)}{d\lambda} G_{ij}(\lambda) d\lambda \quad (18)$$

The half-sinus impuls load:

We consider a half-sinus impuls with a duration Timp and a peak magnitude P₀.

$$f(t) = \begin{cases} P_0 \sin \Omega t & \text{for } 0 \leq t < \pi / \Omega \\ 0 & \text{for } t \geq \pi / \Omega \end{cases}$$

Setting the load function f(t) and the evaluated Green's function G₃₃ and G₁₃ in eq. (18) we obtain for the vertical and radial displacement components W₃₃ and W₁₃ of the half-space surface due to a half-sinus impuls:

$$W_{33}(t) = \int_0^t \frac{df(t-\lambda)}{d\lambda} G_{33}(\lambda) d\lambda \quad (19)$$

$$W_{13}(t) = \int_0^t \frac{df(t-\lambda)}{d\lambda} G_{13}(\lambda) d\lambda \quad (20)$$

where

$$\frac{df(t-\lambda)}{d\lambda} = -\Omega P_0 \cos \Omega(t-\lambda)$$

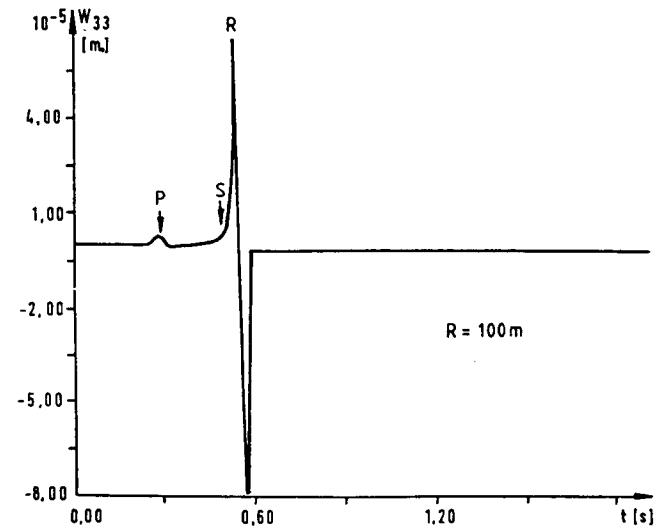
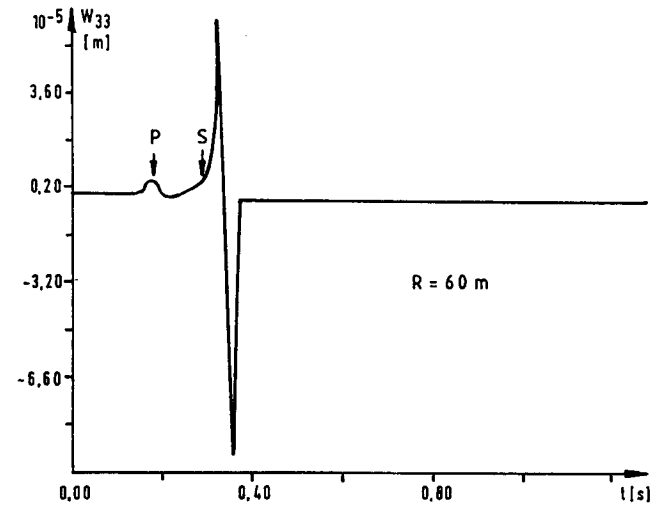
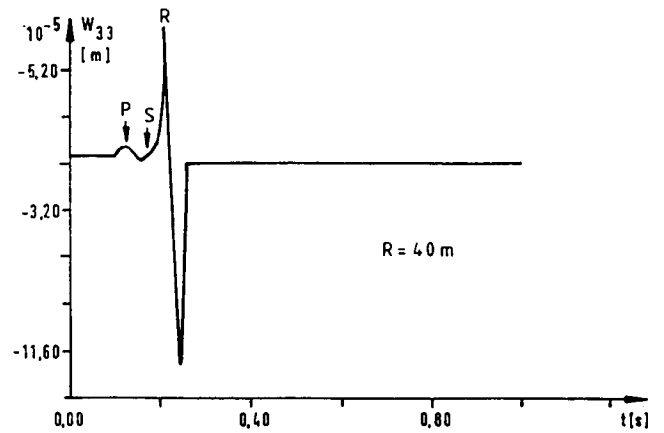


Fig.5 Free field amplitude due to a half-sinus impuls at the surface of the half-space P₀ = 2000 kN; ρ = 1.8 t/m³, ν = 0.33 Timp = 0.05 s

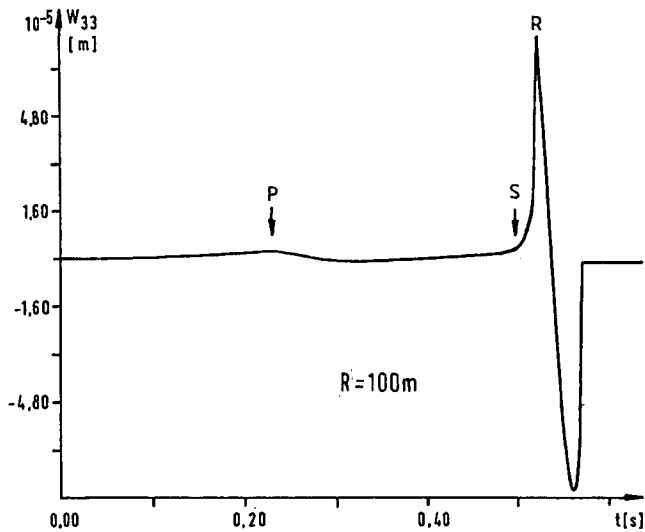
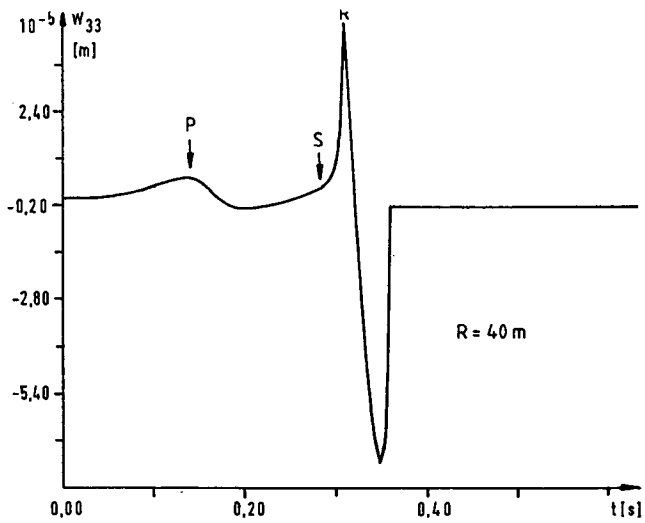
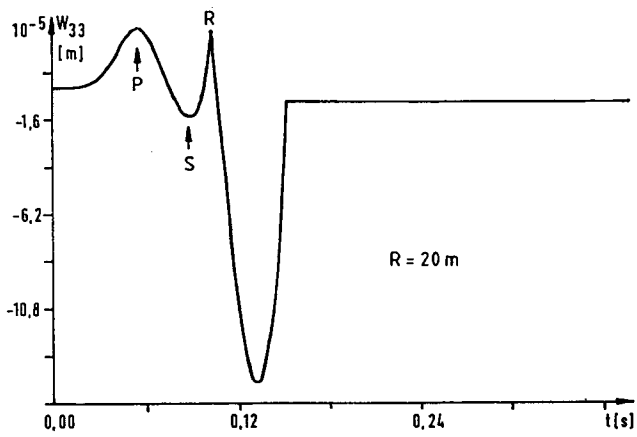


Fig. 6 Free field amplitude due to a half-sinus impuls at the surface of the half-space
 $P_0 = 2000 \text{ kN}$; $\rho = 1.8 \text{ t/m}^3$; $\nu = 0.49$
 $T_{imp} = 0.05 \text{ s}$

Figures 5 and 6 display the graph of the displacement component W_{33} as given by eq. (19) evaluated for various distances R from the source. In both figures we see clearly all the three wave types of the half-space excited at its surface. They are denoted by the symbols P, S and R. The Rayleigh wave is dominant and occurs just after the S-Wave signal.

For materials with great Poisson ratios, Figure 6 ($\nu = 0.49$), as for example water saturated soils, the P-Wave compared to the S-Wave arrives with a considerable strong signal. This phenomenon has been very often neglected in the past years.

Harmonic point load:

We consider a harmonically oscillating vertical load

$$f^H(t) = P \exp(i\Omega t)$$

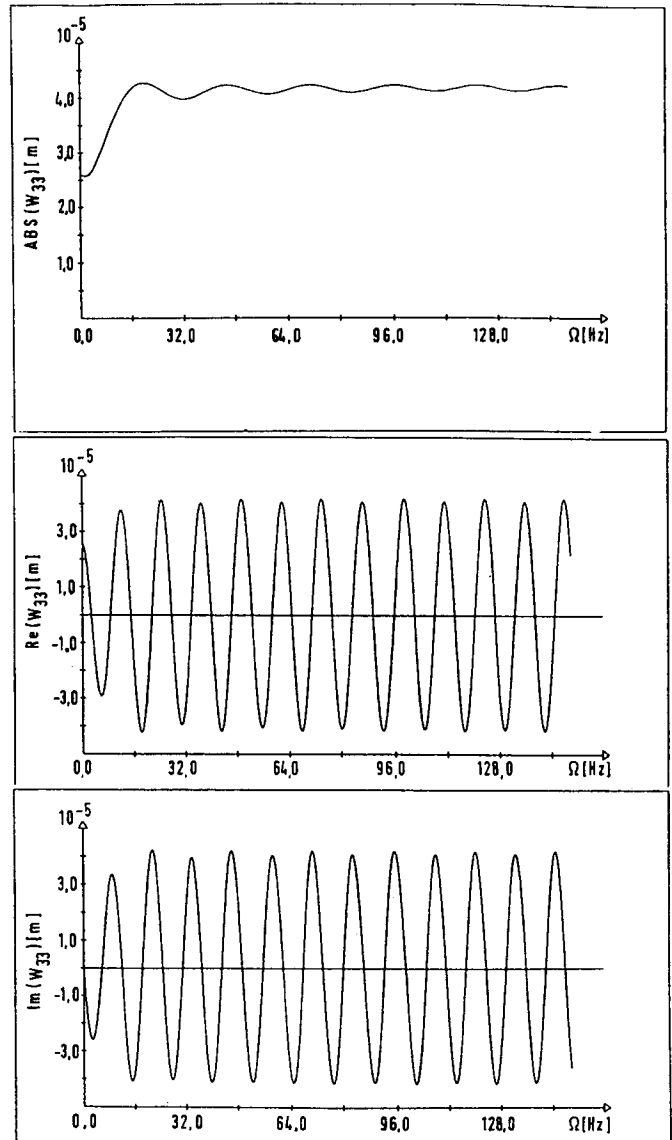


Fig. 7: Free field amplitude due to harmonic load, displacement W_{33}

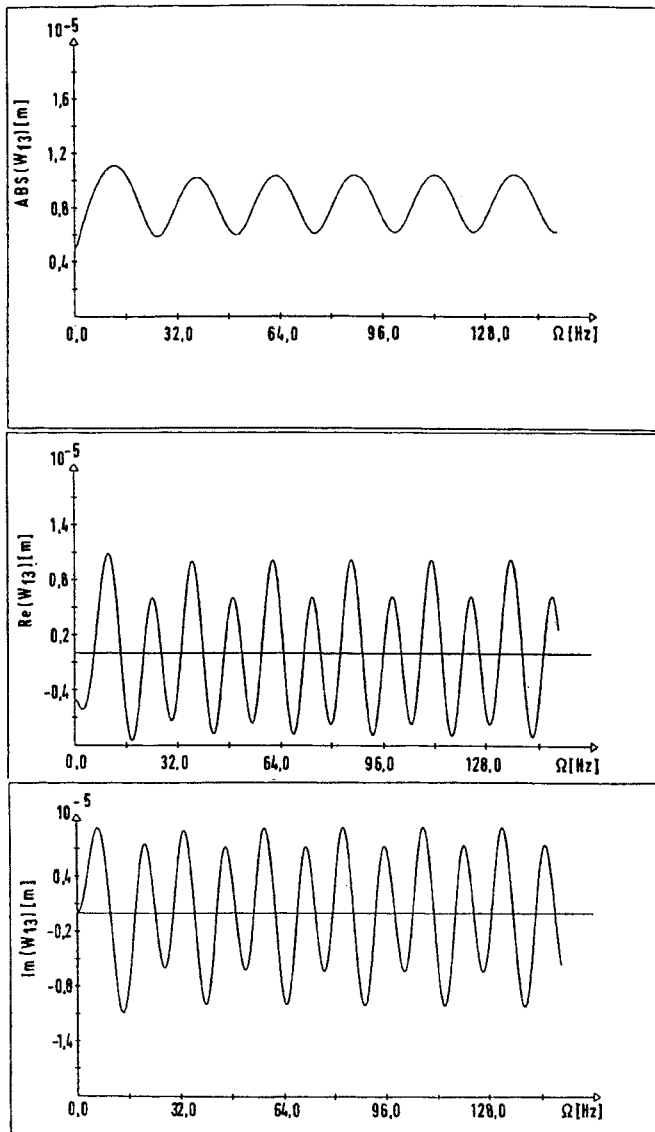


Fig. 8 Free field amplitude due to harmonic load, displacement W_{13}

In order to calculate the system response to the harmonic load we make use again of eq. (18) and we obtain for the two components W_{33} and W_{13}

$$W_{33}(\Omega) = -i\Omega P \int_0^{\infty} \exp(-i\Omega\lambda) G_{33}(\lambda) d\lambda \cdot \exp(i\Omega t) \quad (21)$$

and

$$W_{13}(\Omega) = -i\Omega P \int_0^{\infty} \exp(-i\Omega\lambda) G_{13}(\lambda) d\lambda \cdot \exp(i\Omega t) \quad (22)$$

The integrant in eqs. (21) and (22) represents the steady state oscillation of the half-space surface.

Figures 7 and 8 show the response of the half-space surface due to a harmonic load with amplitude $P = 2000$ kN acting in a depth of $Z_0 = 100$ m in the interior of the half-space. The empirical distance of the control point amounts $R = 20.0$ m.

The considered half-space has a Poisson ratio of $\nu = 0.33$, a density $\rho = 1.8$ t/m³ and the shear wave velocity is $v_s = 200$ m/s.

Figure 7 displays the vertical component W_{33} after eq. (21).

The displacement components are given by their absolute value and the phase to the applied harmonic load is defined by

$$\phi = \arctg \frac{\text{Im}}{\text{Re}} \quad (23)$$

In Figure 8 we see the radial (horizontal) component W_{13} , eq. (22)

MODEL FOR SIMULATION OF PILE DRIVING AND RESULTS

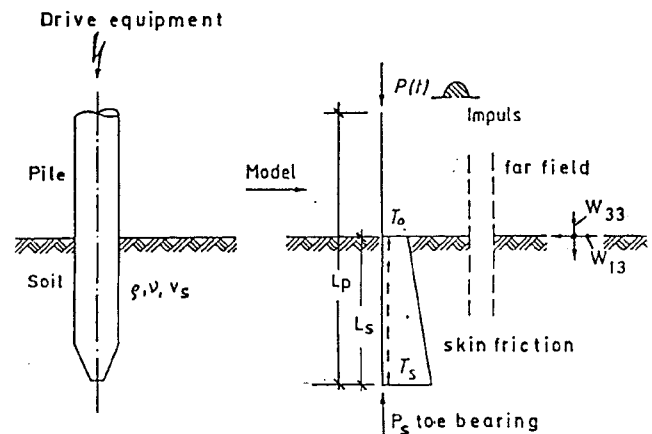


Fig. 9 Simulation model for pile driving - Free field response of the half-space surface

The created solutions for the free field response to a half-sinus impuls, eqs. (19,20), will be used here to simulate the free field response on the surface of a half-space, given by its density ρ , Poisson ration ν and shear wave velocity v_s , due to a pile driving process. The calculated free field response is of practical interest in the far-field. In the near field is the response much more affected by the elasto-plastic phenomena which take place during the driving process and which phenomena cannot be considered by this theoretical solution. The pile considered here has a total length of $L_p = 15.0$ m. The length of the pile shaft in the soil amounts $L_s = 9.0$ m. The skin friction acts along the length L_s with the ordinate T_0 at the surface of

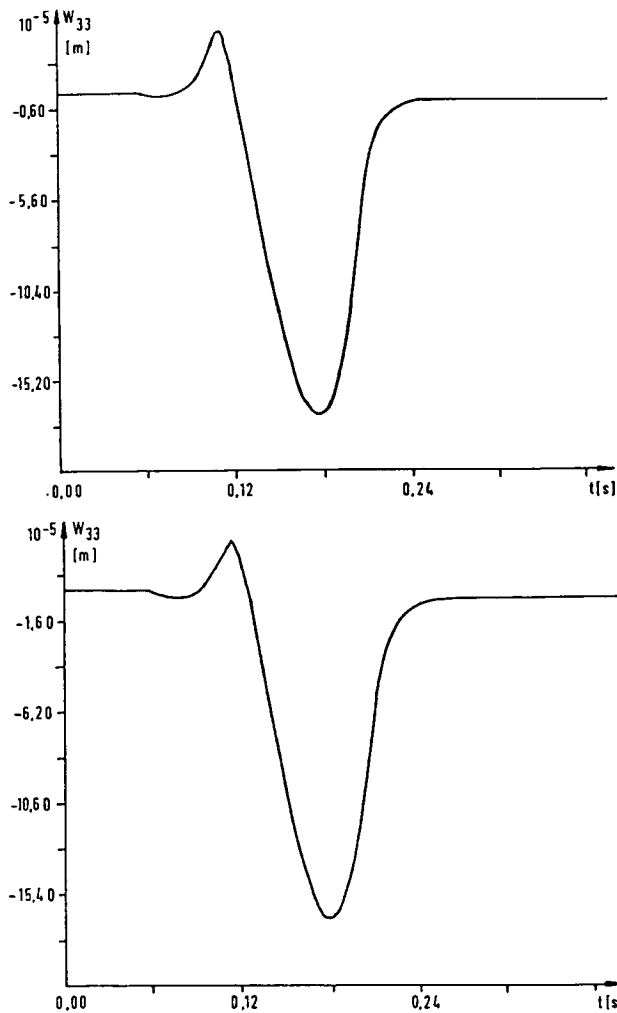


Fig. 10 Free field amplitude $W_{33}(t)$
 a) skin friction 0 %, toe bearing 100%
 b) skin friction 50 %, toe bearing 50%

the half-space and T_S at the pile toe. The ratio T_O/T_S has been chosen to 0.5. At the pile toe acts also the toe bearing capacity P_S . This half-sinus impuls acting at the pile head has a peak magnitude of $P_O = 2000$ kN and its duration amounts $T_{imp} = 0.10$ s. The wave propagation velocity in the pile is $V_A = 4000$ m/s (concrete pile). The sizes ρ , V and v_S for the considered soil are:

$$\rho = 1.8 \text{ t/m}^3; \quad V = 0.33; \quad v_S = 200 \text{ m/s}$$

The influence of the skin friction is here considered by integrating the single-point load solution along L_S by the aid of Gaussian quadrature formula. The time shifting between the impact at the pile head and the Gaussian points along the length L_S has been also considered. The control point at the surface of the soil, where the signals are measured has a distance $R = 20$ m from the pile.

Figure 10a shows the vertical component $W_{33}(t)$ of the displacement on the half-space surface for the theoretical case of non existing skin friction. In Figure 10b the vertical displacement $W_{33}(t)$ is displayed for the case that 50% of the impact magnitude will be emitted from the pile to the soil by skin friction and the other 50 % by the toe bearing capacity.

By comparing both figures we see that skin friction affects the free field magnitude to become larger. This influence of the skin friction is pointed out more clearly in the figures 11a and 11b, which show the horizontal displacement component $W_{13}(t)$. By considering of skin friction, 50 % of the impact magnitude, the free field amplitude is about two times larger as in the case of neglected skin friction.

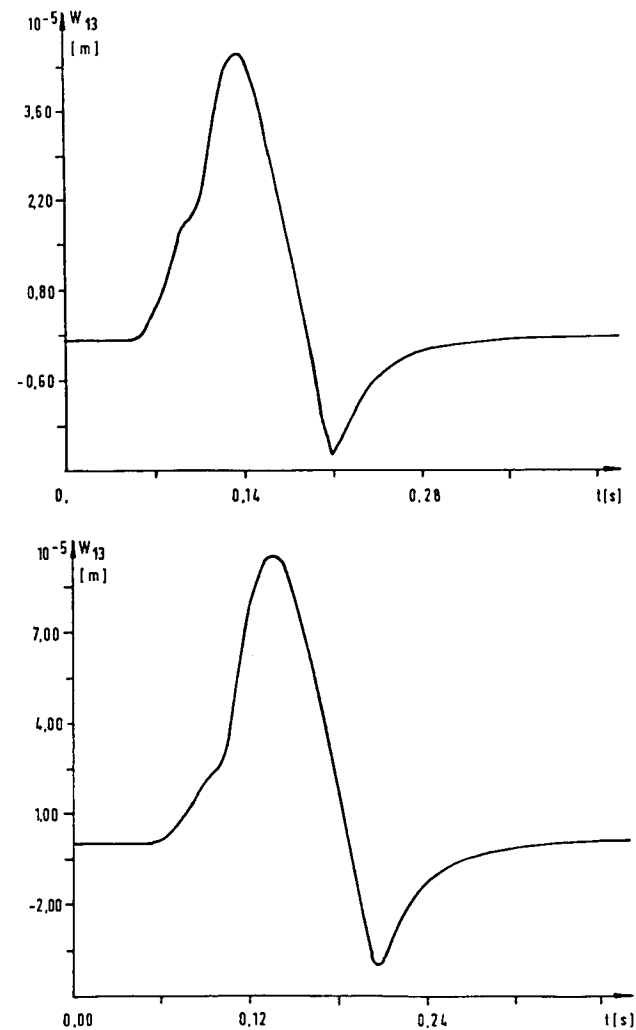


Fig. 11 Free field amplitude $W_{13}(t)$
 a) skin friction 0%, toe bearing 100%
 b) skin friction 50%, toe bearing 50 %

CONCLUSIONS

The phenomenon of wave propagation in the soil is described by so called Green's function. These solutions, gained by analytical methods, are numerically very stable and thus extremely suitable for investigations in various practical application purposes. By use of the Green's functions the authors calculated the free-field response of the half space due to various loads acting in the interior of the half-space or at its surface, as half sinus impuls or harmonic point load. Finally a pile driving process has been simulated. The outhors investigated the influence of some substantial parameters as skin friction and the toe bearing capacity of the pile.

REFERENCES

- Johnson, L.R. (1974), "Green's Functions for Lamb's Problem" Geophys. Jour. Royal Astr. Society, Vol. 37, 99-131
- Mitakidis, A. (1989) "Zur analytischen Lösung des Problems der dreidimensionalen Wellenausbreitung im elastischen Halbraum mit Anwendung auf dynamische Randwertprobleme" Dissertation 1989, Fachbereich Bauingenieur- und Vermessungswesen, Technische Universität Berlin